

# Coexistence but Independent Biosynthesis of Catechyl and Guaiacyl/Syringyl Lignin Polymers in Seed Coats<sup>WJOPEN</sup>

Yuki Tobimatsu,<sup>a,1</sup> Fang Chen,<sup>b,c,1,2</sup> Jin Nakashima,<sup>b</sup> Luis L. Escamilla-Treviño,<sup>b,c,2</sup> Lisa Jackson,<sup>b,c</sup> Richard A. Dixon,<sup>b,c,2</sup> and John Ralph<sup>a,d,3</sup>

<sup>a</sup> Department of Biochemistry, University of Wisconsin–Madison, Wisconsin Energy Institute, Madison, Wisconsin 53726

<sup>b</sup> Plant Biology Division, Samuel Roberts Noble Foundation, Ardmore, Oklahoma 73401

<sup>c</sup> U.S. Department of Energy, BioEnergy Sciences Center, Oak Ridge National Laboratory, Oak Ridge, Tennessee 37831

<sup>d</sup> U.S. Department of Energy, Great Lakes Bioenergy Research Center, Wisconsin Energy Institute, Madison, Wisconsin 53726

ORCID ID: 0000-0002-6093-4521 (J.R.).

**Lignins are phenylpropanoid polymers, derived from monolignols, commonly found in terrestrial plant secondary cell walls. We recently reported evidence of an unanticipated catechyl lignin homopolymer (C lignin) derived solely from caffeyl alcohol in the seed coats of several monocot and dicot plants. We previously identified plant seeds that possessed either C lignin or traditional guaiacyl/syringyl (G/S) lignins, but not both. Here, we identified several dicot plants (Euphorbiaceae and Cleomaceae) that produce C lignin together with traditional G/S lignins in their seed coats. Solution-state NMR analyses, along with an in vitro lignin polymerization study, determined that there is, however, no copolymerization detectable (i.e., that the synthesis and polymerization of caffeyl alcohol and conventional monolignols in vivo is spatially and/or temporally separated). In particular, the deposition of G and C lignins in *Cleome hassleriana* seed coats is developmentally regulated during seed maturation; C lignin appears successively after G lignin within the same testa layers, concurrently with apparent loss of the functionality of O-methyltransferases, which are key enzymes for the conversion of C to G lignin precursors. This study exemplifies the flexible biosynthesis of different types of lignin polymers in plants dictated by substantial, but poorly understood, control of monomer supply by the cells.**

## INTRODUCTION

Phenylpropanoids constitute a diverse group of Phe-derived secondary metabolites that accumulate in various plant tissues as monomeric, oligomeric, or polymeric compounds with a multitude of biological and physiological functions (Vogt, 2010). Lignin is an especially abundant phenylpropanoid polymer produced by the oxidative polymerization of *p*-hydroxycinnamyl alcohols (monolignols). Lignins are major components of secondary cell walls produced in various plant tissues and are particularly abundant within vascular tissues where they confer structural support, vascular integrity, and pathogen resistance. Lignin biosynthesis is a highly conserved trait and its variability is considered to correlate closely with the diversity and evolution of land plants (Boerjan et al., 2003; Bonawitz and Chapple, 2010; Vanholme et al., 2010a; Weng and Chapple, 2010). Perturbing lignin biosynthesis and bioengineering of lignins have attracted significant research attention mainly because lignin hinders many agro-industrial

processes, such as those that generate pulp or biofuels from lignocellulosic plant biomass (Chen and Dixon, 2007; Vanholme et al., 2008, 2012; Weng et al., 2008; Mansfield, 2009; Simmons et al., 2010; Carpita, 2012; Bonawitz and Chapple, 2013).

The monolignol biosynthetic pathway involves functionalization of pathway intermediates by aromatic hydroxylation and O-methylation (as well as successive side-chain reductions) to finally generate monolignols differing in their degree of methoxylation (see Supplemental Figure 1 online). Lignin composition, which is primarily determined by monolignol availability, shows a wide variability among taxa, cell types, and individual cell wall layers and is also influenced by developmental and environmental factors (Boerjan et al., 2003; Bonawitz and Chapple, 2010; Vanholme et al., 2010a; Weng and Chapple, 2010). In general, lignins found in the stem tissues are copolymers composed only of *p*-hydroxyphenyl (H), guaiacyl (G), and syringyl (S) units, which are biosynthesized by polymerization of *p*-coumaryl, coniferyl, and sinapyl alcohols, but essentially lack catechyl (C) and 5-hydroxyguaiacyl (5H) units that may, in principle, derive from participation of caffeyl and 5-hydroxyconiferyl alcohols in lignification (see Supplemental Figure 1 online). Until recently, those units were only identified in abnormal lignins in transgenic plants in which either of the genes for the two O-methyltransferases (CCoAOMT and COMT; see Supplemental Figure 1 online) in the monolignol pathway had been downregulated (Marita et al., 2001; Ralph et al., 2001a; Vanholme et al., 2010b; Weng et al., 2010; Wagner et al., 2011).

Relative to vascular tissues, the structure and biosynthesis of lignins in plant seeds have received little attention. During seed development, the ovule integuments differentiate into several tissue

<sup>1</sup> These authors contributed equally to this work.

<sup>2</sup> Current address: Department of Biological Sciences, University of North Texas, 1155 Union Circle, Denton, TX 76203.

<sup>3</sup> Address correspondence to jralph@wisc.edu.

The authors responsible for distribution of materials integral to the findings presented in this article in accordance with the policy described in the Instructions for Authors ([www.plantcell.org](http://www.plantcell.org)) are: John Ralph (jralph@wisc.edu) and Richard A. Dixon (Richard.Dixon@unt.edu).

<sup>WJOPEN</sup> Online version contains Web-only data.

<sup>OPEN</sup> Articles can be viewed online without a subscription.

[www.plantcell.org/cgi/doi/10.1105/tpc.113.113142](http://www.plantcell.org/cgi/doi/10.1105/tpc.113.113142)

layers composed of different specialized cells to form the protective seed coat (testa) (Haughn and Chaudhury, 2005; Debeaujon et al., 2007; Bewley et al., 2013). Some testa cells develop heavily lignified secondary cell walls where lignins are thought to reinforce the cell and make the seed coat impermeable to water and gasses (Rolston, 1978; Egley et al., 1983; Kelly et al., 1992; Liang et al., 2006). Recently, we reported evidence that lignins (or lignin-like polymers) synthesized specifically in the seed coats of the vanilla orchid (a monocot) are naturally biosynthesized solely from caffeyl alcohol, producing a rather remarkable C lignin homopolymer with essentially only one type of structural unit (Chen et al., 2012). A subsequent survey of 130 different cactus species revealed that many members of the Cactaceae (dicots) also possess seed coat lignins of the C lignin type, whereas others possess normal guaiacyl/syringyl (G/S) lignins (Chen et al., 2013). Surprisingly, a few species contained 5H units in their seed coats. Although it remains to be determined whether C lignin is more widespread throughout the plant kingdom, our data so far imply that the possession of C lignin is not an ancient trait and may have evolved recently, and probably frequently, within different plant lineages.

NMR techniques resolved the uniquely defined structure of the C lignin in the seed coats as being composed almost exclusively of benzodioxane units, with linkages derived from  $\beta$ -O-4-type end-wise radical coupling reactions that typify lignification, that is, in which the main reaction is coupling of a caffeyl alcohol radical, at its  $\beta$ -position, with the radical of the catechol end unit, at its 4-O-phenolic position, of the growing polymer (Chen et al., 2012). An intriguing observation was that all the C lignins identified to date were generally composed only of caffeyl alcohol-derived units with no evidence for the presence of classical G or S lignin units derived from coniferyl or sinapyl alcohols in the same seed coats. Within our survey, by contrast, lignins produced in vegetative tissues in those plants were always composed of mixtures of G and S units without any trace of C units (Chen et al., 2013).

Here, we describe the presence and structure of C lignins in seed coats of another set of dicotyledonous angiosperm plants, namely, members of the Euphorbiaceae and Cleomaceae families. Unlike previously studied plants, these plants appear to possess C lignin together with classical G/S or G lignins in the same seed coat organs. We used NMR analysis of seed cell wall structures and *in vitro* lignin polymerization studies to determine whether these plant seed lignins are heterogeneous copolymers or discrete C and G/S polymers and to therefore delineate whether they are biosynthesized concurrently or independently. The findings, supported by biochemical and morphological analysis of developing cleome seeds, demonstrate a tightly regulated process for the biosynthesis of monomers and their targeting to cell walls during seed maturation where their assembly to lignin polymers remains under simple chemical control.

## RESULTS

### Identification of C Lignin with G/S or G Lignin Polymers in Plant Seeds

Analysis of lignin monomer composition by thioacidolysis indicated that lignins in the seed coats of several members of the

Euphorbiaceae and Cleomaceae contain high levels of caffeyl alcohol-derived C units, whereas others contain only typical G and/or S lignin units or very low lignin amounts (Figure 1). Unlike in the plants previously studied (mainly members of the Orchidaceae and Cactaceae), the seed coats of the plants with C units also contain significant portions of G and/or S units derived from coniferyl and/or sinapyl alcohols; some of the members contain C units together with only G units, and some others additionally contain S units. Analysis of cell wall preparations from stem, leaves, and roots from one Euphorbiaceae plant (*Ricinus communis*) indicated, not surprisingly, that the lignin in vegetative tissues was composed of G and S units without any trace of C units (see Supplemental Figure 2 online).

Entire seed coat tissues from mature seeds of selected species of Euphorbiaceae (*Jatropha curcas*, *Vernicia fordii*, and *Aleurites moluccana*) and Cleomaceae (*Cleome hassleriana*) plants were further analyzed by wet-chemical and solution-state two-dimensional NMR analyses. Klason analysis showed high levels of acid-insoluble lignins in these seeds (50 to 70%); the majority of the remaining materials appeared to be typical cell wall polysaccharides, such as crystalline cellulose and hemicelluloses mainly composed of xylans with lesser amounts of glucans and arabinans (Table 1). In the heteronuclear single quantum coherence (HSQC) NMR spectra of entire plant seed coats (Figure 2), acquired via the dissolution/acetylation method (Lu and Ralph, 2003; Mansfield et al., 2012), aromatic signals from the etherified (C) and nonetherified (C') catechyl rings were clearly observed together with the signals from the typical G/S lignin units (G and/or S), showing that either both types of lignins, or copolymer lignins, are present in these tissues. Volume integration of the contour signals allowed reasonable quantifications of 40 to 60% C units, with the rest being typical G/S lignin units. The NMR-derived C lignin levels are substantially higher than the values estimated from the released thioacidolysis monomers (Figure 1), reasonably because C lignin polymers mainly comprised of atypical  $\beta$ -ether-linked units (benzodioxanes; see below) are substantially resistant to thioacidolysis treatments (Marita et al., 2003; Moinuddin et al., 2010). The apparently high ratio of nonetherified C endgroups (C') to etherified C units (C) is almost certainly anomalous due to the different NMR relaxation behaviors of the more mobile end units compared with the rigid internal units; this contention is confirmed below by molecular mass analysis.

The aliphatic side-chain regions of the NMR spectra (Figure 2) resolve most of the correlations for the various lignin interunit linkage types as well as the typical cell wall polysaccharides (e.g., glucans, xylans, and arabinans), as we also identified by wet-chemical methods (Table 1). In all the plant seed spectra, the two predominant lignin linkage types are acyclic  $\beta$ -aryl ether units I and benzodioxane units IV, both derived from  $\beta$ -O-4-type radical coupling reactions that typify lignification; the former arise from coupling (at the  $\beta$ -position) of any of the hydroxycinnamyl alcohol monomers with a guaiacyl or syringyl unit (at the 4-O-position) via a pathway involving external nucleophilic water addition to the quinone methide intermediate (Figure 3A), and the latter likewise but uniquely from coupling (at the  $\beta$ -position) of any of the hydroxycinnamyl alcohol monomers with a catechyl end unit (derived from incorporation of caffeyl alcohol, at the 4-O-position) via a new pathway (Chen et al., 2012) involving intramolecular

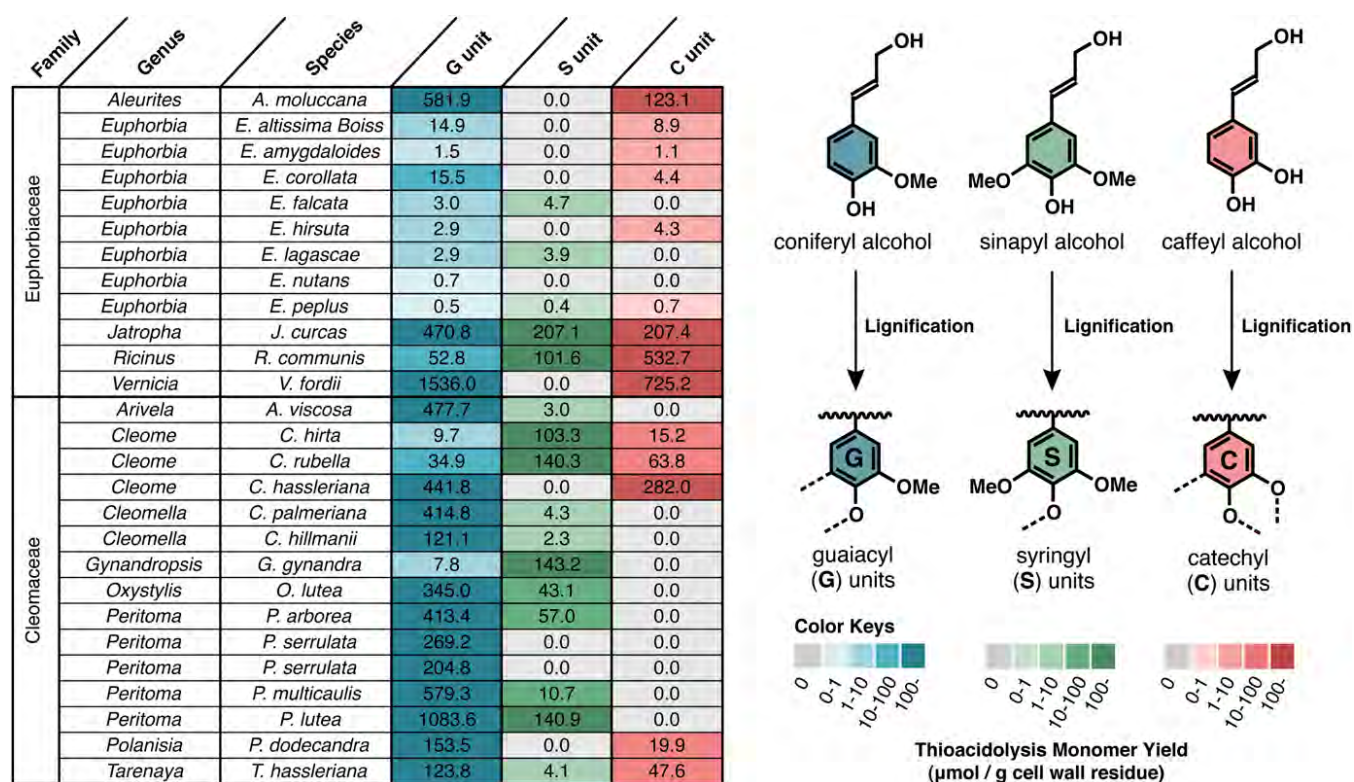


**Figure 1.** Seed Coat Lignin Compositions of Euphorbiaceae and Cleomaceae Plants.

Values and color coding show yields of monomeric guaiacyl (G), syringyl (S), and catechyl (C) type trithioethylpropylphenols ( $\mu\text{mol}/\text{g}$  cell wall residues) released by analytical thioacidolysis treatments of mature plant seeds.

quinone methide trapping by the 3-OH in catechyl units (Figure 3B). Analogous benzodioxanes have also been authenticated as products of lignification with other atypical lignin precursors, including precursors with *o*-diphenolic structures, such as 5-hydroxyconiferyl alcohol (Ralph et al., 2001b; Lu et al., 2010; Vanholme et al., 2010b; Weng et al., 2010), rosmarinic acid (Tobimatsu et al., 2012), and galocatechin derivatives (Elumalai et al., 2012), either *in vivo*, *in vitro*, or both. The challenge (below) is to determine whether the lignins being measured in the seed coats of the Euphorbiaceae and Cleomaceae plants are copolymers of all units (C, G, and S) or result from independent coupling of caffeyl alcohol to form C lignin and separate, conventional polymerization of coniferyl and sinapyl alcohols. Less abundant but clear signals from phenylcoumaran **II** and resinol **III** units were also observed in the HSQC spectra; these are most likely generated via classical lignin polymerization of coniferyl and sinapyl alcohols, although polymerization of caffeyl alcohol itself also produces these units as trace components in the resulting C lignin (Chen et al., 2012).

#### Direct Connections between C Lignin and G/S Lignin Polymers in Plant Seeds?

In order to delineate whether the lignins are actually C-G/S lignin copolymers or independent polymers, NMR experiments that determine the connectivity between lignin units are required, along with model studies to determine if copolymerization results

when all monomers are present. The former experiments are difficult on whole-cell-wall samples due to their rapid NMR relaxation, so lignin isolation was used to obtain cleaner samples with better relaxation characteristics. Soluble pure lignin fractions were isolated via treatment of ball-milled seed coats with crude cellulases followed by extraction with 96% dioxane:water solution (Björkman, 1954; Ralph et al., 2006; Stewart et al., 2009; Chen et al., 2012). HSQC spectra confirmed the successful removal of the polysaccharides and concurrent enrichment of lignins (see Supplemental Figure 3 online) and displayed similar distributions of lignin aromatics (Figure 4A) as observed in the spectra of entire seed coat tissues (Figure 2).

Heteronuclear multiple-bond correlation (HMBC) spectra resolved the long-range correlations between lignin side-chain protons and aromatic ring carbons revealing their direct connectivities (Figures 4B and 4C). In all the plant seed lignin spectra, the correlations from  $\alpha$ -protons in *trans*-benzodioxane units **IV**, which are derived only from cross-couplings of a monomer to C polymer end units, are predominantly/exclusively to C rings and essentially lack correlation signals to G and S rings (Figure 4B). This implies that the benzodioxane units are majorly/exclusively derived from homopolymerization of caffeyl alcohol. Moreover, the correlations from  $\alpha$ -protons in  $\beta$ -aryl ether units **I**, which are derived from cross-couplings of a monomer onto G or S polymer units, are only observed to G and S rings, and there is no evidence for correlations to C rings (Figure 4C). Again, this implies that the coupling to G and

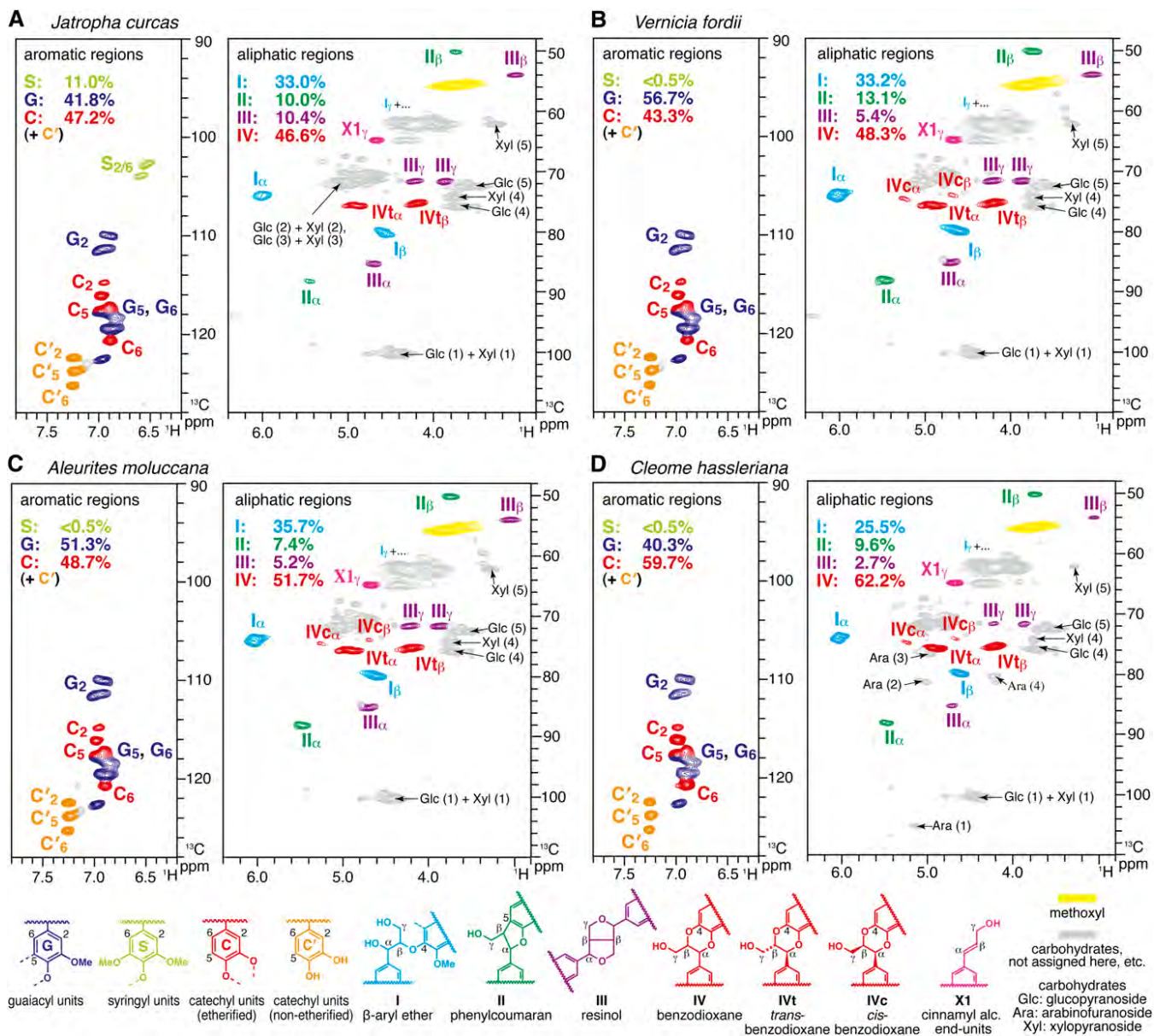


**Figure 2.** Short-Range  $^{13}\text{C}$ - $^1\text{H}$  Correlation (HSQC) NMR Spectra of Plant Seed Coat Cell Walls.

Whole seed coat cell wall preparations from mature seeds of *J. curcas* (A), *V. fordii* (B), *A. moluccana* (C), and *C. hassleriana* (D). Aromatic and aliphatic subregions are displayed. Volume integrals are given for the lignin aromatic units and side-chain structures that are color-coded to match their assignments in the spectrum.

S units is only by the G and S monomers, coniferyl and sinapyl alcohol, and not by the C monomer, caffeyl alcohol. Thus, within the limits of NMR detection, there is no evidence for direct linkages between C lignin and G/S lignins present in the plant seed coats.

### In Vitro Lignin Copolymerization Generates G/S/C or G/C Copolymers

We performed in vitro peroxidase-catalyzed copolymerization of caffeyl alcohol with coniferyl and sinapyl alcohols to test whether

caffeyl alcohol, the monolignols, and their oligomers are capable of cross-coupling with each other in a typical lignin polymerization. HSQC NMR spectra of the resultant synthetic lignins (dehydrogenation polymers [DHPs]) confirmed, by exhibiting the characteristic signals from the monomeric units, successful incorporation of each precursor into lignin polymers (Figure 4A; see Supplemental Figure 4 online).

HMBC spectra of the DHPs, in contrast with the plant seed lignin spectra, displayed clear correlations showing the direct connectivity between the benzodioxane side chains and G/S

**Table 1.** Chemical Compositions of Euphobiaceae and Cleomaceae Seed Coats

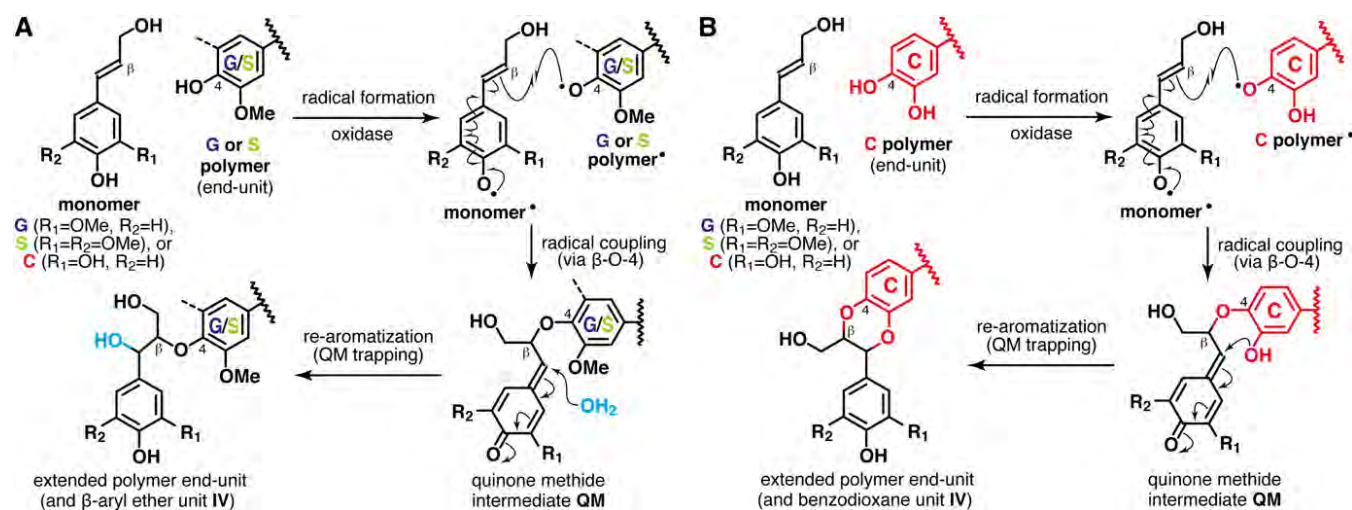
Component	<i>J. curcas</i>	<i>V. fordii</i>	<i>A. moluccana</i>	<i>C. hassleriana</i>
Klason lignin (mg/g)	480.8	686.0	604.8	460.0
Glc, crystalline; cellulose (mg/g)	261.2	126.7	211.0	201.9
Glc, amorphous (mg/g)	8.4	3.9	8.7	6.8
Rhamnose (mg/g)	2.7	1.1	1.4	4.4
Fucose (mg/g)	0.2	0.2	0.2	0.7
Arabinose (mg/g)	4.8	3.6	3.9	21.7
Xylose (mg/g)	222.6	137.7	168.3	86.6
Mannose (mg/g)	6.2	1.8	2.0	4.1
Gal (mg/g)	8.2	5.5	5.9	10.8
Ash (mg/g)	0.6	1.0	0.8	4.7

aromatic rings (Figure 4A) and also between the  $\beta$ -aryl ether side chains and C aromatic rings (Figure 4B). Thus, all three monomers are capable of cross-coupling with all three unit types (C, G, and S) when present together during the polymerization process. A major difference between the synthetic copolymers and the plant seed lignins was also seen in the aromatic regions of their HSQC spectra (Figure 4A). The signals from catechyl end-unit correlations (C) were not observed in the DHP spectra, whereas they are clearly seen in all the plant seed lignins (Figures 4B and 4C). This suggests that, in the synthetic lignins derived from the C monomer and G/S monomers, free catechyl end units were efficiently capped by coniferyl and/or sinapyl alcohol monomers through cross-coupling reactions, generating benzodioxanes and not leaving catechyl units at the ends of the chains. We previously noted, in synthetic coupling reactions and from metabolite profiling (Morreel et al., 2004; Lu et al., 2010), that the analogous 5-hydroxyconiferyl alcohol cross-products never retain the reactive catechyl end group during polymerization. The HSQC observation (Figure 4A) is completely consistent with the HMBC spectra showing signals from G- or S-connected

benzodioxanes more clearly than those from C-connected benzodioxanes in these synthetic copolymer lignins (Figure 4B). Overall, these *in vitro* experiments further support the contention that caffeoyl alcohol polymerization in plant seeds is spatially and/or temporally separated from polymerization of coniferyl and sinapyl alcohols, producing physically distinct homopolymer C lignin and heteropolymer G/S lignins within the seed coat.

#### Molecular Mass Distributions of Seed Coat Lignin Polymers

We also performed gel permeation chromatography (GPC) to determine molecular mass distributions of the lignin polymers (Figure 5; see Supplemental Table 1 online). The acetylated samples of the ball-milled seed coat tissues and the dioxane-soluble lignins isolated from them have wide molecular mass distributions in the range up to  $10^6$  D based on polystyrene standards. The number-average molecular masses of the whole seed coat tissues vary between 5 and 10 kD, whereas the corresponding isolated lignins appeared to have lower molecular

**Figure 3.** Generation of Major Lignin Units by  $\beta$ -O-4-Type End-Wise Radical Coupling Reactions.

**(A)** Conventional pathway for  $\beta$ -aryl ethers via cross-coupling of a hydroxycinnamyl alcohol monomer onto guaiacyl (G) or syringyl (S) polymer end units.

**(B)** Novel pathway for benzodioxanes via cross-coupling of a monomer onto catechyl (C) polymer end units.

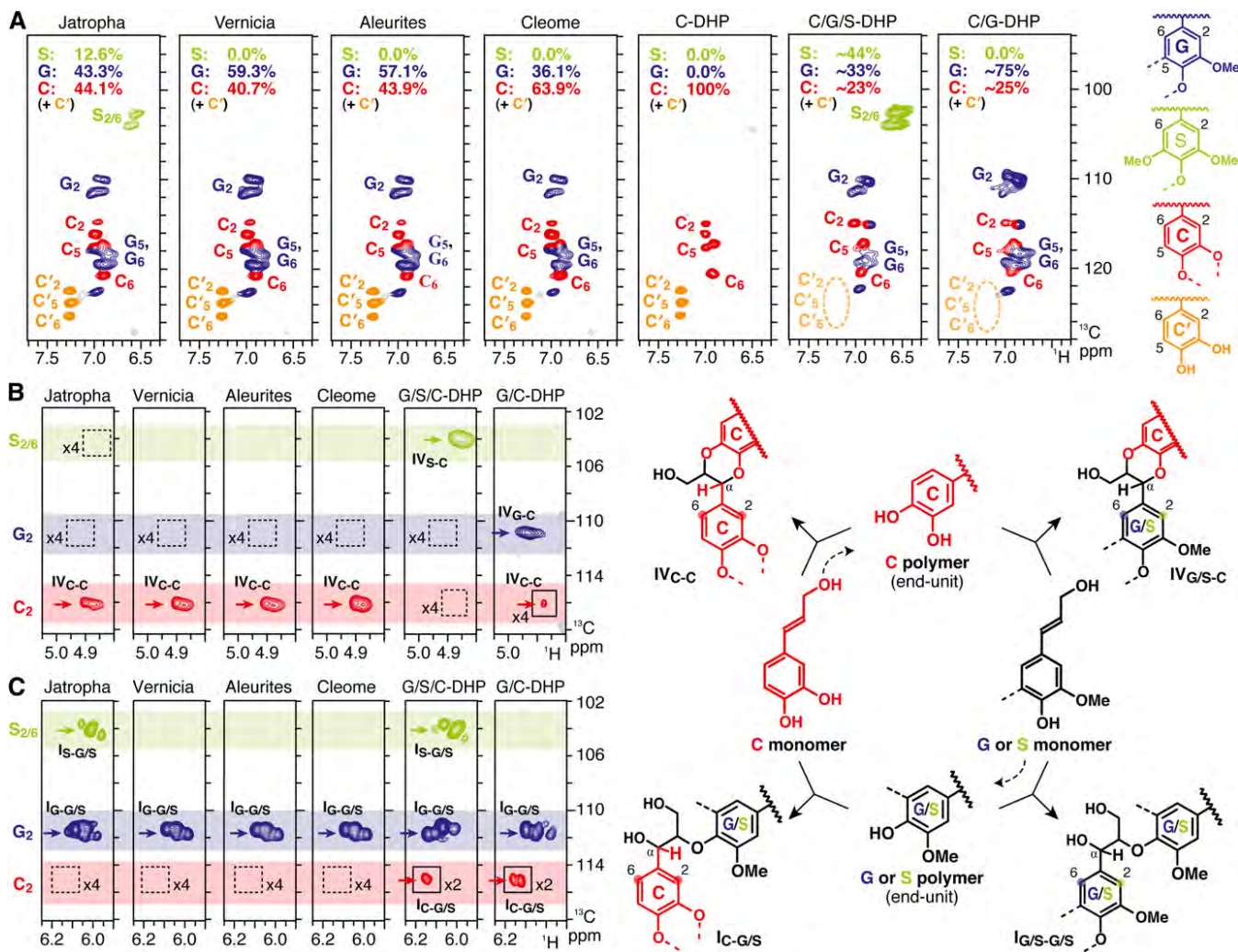


**Figure 4.** NMR Characterization of Isolated Plant Seed Coat Lignins and in Vitro Synthetic Lignin Polymers (DHPs).

**(A)** Aromatic subregions of short-range  $^{13}\text{C}$ - $^1\text{H}$  correlation (HSQC) NMR spectra. Volume integrals are given for the lignin aromatic units that are color-coded to match their assignments in the spectrum.

**(B)** and **(C)** Partial long-range  $^{13}\text{C}$ - $^1\text{H}$  (HMBC) NMR spectra, showing subregions exhibiting aromatic correlations to benzodioxane  $\alpha$ -protons **(B)** and correlations to  $\beta$ -aryl ether side-chain  $\alpha$ -protons **(C)**. Box with x2 or x4 indicates regions that were vertically scaled two- or fourfold.

masses, 3 to 5 kD; it is most plausible that the insoluble fractions left after lignin extractions contain the polymers with higher molecular masses. The averaged molecular masses of the synthetic lignins, DHPs, were even lower than those of the isolated lignins, 2 to 3 kD, which is consistent with previous studies comparing the molecular masses of conventional DHPs and those of lignins isolated from plants (Faix et al., 1981; Cathala et al., 2003; Tobimatsu et al., 2006). Interestingly, it appears that addition of caffeoyl alcohol into the monomer mixtures lowers the molecular masses of the coniferyl alcohol-based DHPs. In our previous report comparing the molecular masses of C lignin and G/S lignins separately isolated from *Vanilla planifolia* seed coats and stems, the former likewise has a lower average molecular mass than that of the latter (Chen et al., 2012). These may imply a slightly lower polymerization capability of caffeoyl alcohol than those of

traditional monolignols, both in vitro and in vivo; the lower molecular masses of C lignins may be attributable to the strong tendencies for the monomer toward the end-wise  $\beta$ -O-4 coupling reaction to make the linear polymer, excluding polymer-polymer coupling reactions via the other possible coupling modes such as 5-5 and 4-O-5 couplings that are typically seen in the polymerization of growing oligomers from the traditional monolignols (Yue et al., 2012). Overall, all the molecular mass data presented here are within the range of literature values reported for various in vitro and in vivo lignins using similar analytical methods (Tobimatsu et al., 2006; Holtman et al., 2007; Chen et al., 2012; Rencoret et al., 2013). We also confirmed that all the lignin samples elute earlier (i.e., represent higher molecular mass material) than authentic acetylated caffeoyl alcohol monomer (molecular mass = 292) and the benzodioxane dimer (molecular mass = 498) (Figure 5).

Collectively, these observations support our contention that all the information drawn by NMR and other chemical methods here reflect structural characteristics of polymeric lignins present in the plants.

### Developmentally Regulated Lignin Deposition during Cleome Seed Maturation

To determine whether C lignin deposition is temporally separated from G/S lignin deposition in plant seed coats, time courses of lignin deposition during seed development in *C. hassleriana* plants were investigated by analytical thioacidolysis. In addition, we measured extractable *O*-methyltransferase (OMT) enzyme activities in developing *C. hassleriana* seeds, as these are considered to be the key enzymes for conversion of lignin precursors from the C to the G/S aromatic levels (see Supplemental Figure 1 online).

During seed development, thioacidolysis-derived G lignin signatures appeared shortly after pollination, rapidly increased, and reached a plateau at around 12 d after pollination (DAP), before which time no C lignin signatures were detected (Figure 6A). C lignin signatures first appeared at 14 DAP, when the seed coat starts to darken, and then rapidly developed over the next 6 d, by which time the seed coats became dark and hard (Figure 6A; see Supplemental Figure 5 online). Deposition of C and G lignins are therefore at least temporally separated during *C. hassleriana* seed development. Furthermore, it was clearly observed that

extractable OMT activities, expressed independently as CCoAOMT and COMT activities based on the dry seed weights, abruptly drop after 14 DAP, when G lignin deposition completes and C lignin starts accumulating (Figure 6B), whereas total extractable protein levels in seeds remain constant during 12 to 14 DAP (for OMT activities based on protein content; see Supplemental Figure 6 online). As further discussed below, it is therefore apparent that the developmental transition from G to C lignins is, at least in part, modulated by expression of OMTs involved in the conversion of C precursors into G precursors.

### Lignin Localization in Developing Cleome Seeds

Finally, to attempt to determine whether or not syntheses of C and G lignins occur in the same cell walls, lignin deposition during *C. hassleriana* seed maturation was visualized by microscopy coupled with histochemical lignin staining methods. The *C. hassleriana* seed coat possesses two continuous layers of thick, lignified cells beneath the exotestal cells. Both of these display intense autofluorescence and deep blue and pinkish colorations upon conventional lignin staining with toluidine blue O and phloroglucinol-hydrochloric acid at 20 DAP when lignification has been completed (Figure 6C, pictures in the top three rows). The outer main sublayer (indicated by yellow arrows) apparently undergoes cell wall thickening and lignification earlier than the inner sublayer (indicated by orange arrows). In the outer main sublayer, mature cells with thick lignified walls are already apparent at 9

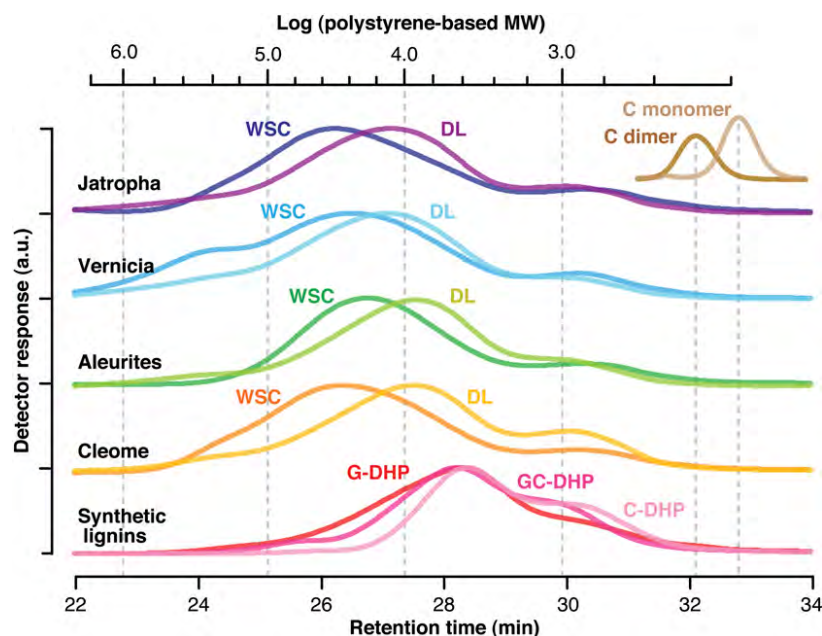


**Figure 5.** GPC Elution Profiles of Plant Seed Coat Lignins, Synthetic Lignin Polymers (DHPs), Synthetic Catechyl Benzodioxane Dimer (C-Dimer), and Caffeyl Alcohol Monomer (C-Monomer).

Ball-milled whole seed coat cell wall preparations (WSC) and dioxane-soluble lignins (DL) were prepared from mature seeds of the plants indicated. DHPs were prepared via *in vitro* peroxidase-catalyzed polymerization of coniferyl alcohol (G-DHP), caffeyl alcohol (C-DHP), and caffeyl alcohol with coniferyl alcohol (G/C-DHP). C-dimer (molecular mass = 498) was synthesized via oxidation of C-monomer (molecular mass = 292) using silver carbonate. All the lignin samples and model compounds were acetylated prior to GPC analysis. Scale bar at the top indicates the logarithmic range of the molecular masses of polystyrene standards. Polystyrene-based molecular mass data are listed in Supplemental Table 1 online. a.u., arbitrary unit.

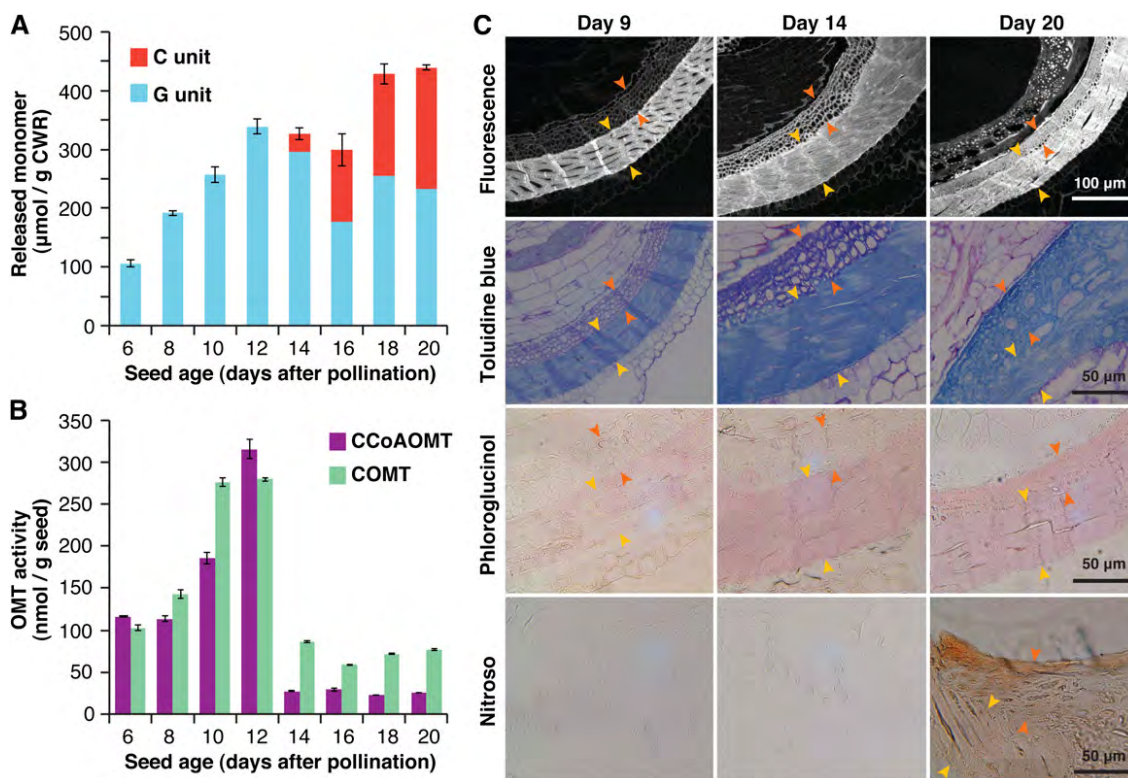


**Figure 6.** Lignin Deposition during *C. hassleriana* Seed Coat Development.

**(A)** Seed lignin compositions determined by thioacidolysis. Yields of guaiacyl (G) and catechyl (C) type trithioethylpropylphenols ( $\mu\text{mol/g}$  cell wall residues [CWR]) released from the seed coat cell wall preparations are plotted against seed ages (days after pollination).

**(B)** Extractable CCoAOMT and COMT activities in crude protein extracts from the seeds. Enzyme activity is expressed based on dry seed weight.

**(C)** Transverse seed sections imaged directly by phenolic autofluorescence or by histochemical lignin staining with toluidine blue O or phloroglucinol-HCl for detection of both G and C lignins or with nitroso reagent for selective detection of C lignin. The two distinguishable sublayers of lignified cells (indicated by yellow and orange arrows) are visible beneath the exotestal cell layers.

DAP, and these becomes denser at 14 and 20 DAP during the period when both G and C lignins are deposited (as determined by thioacidolysis; Figure 6A). In the inner sublayer, immature cells with relatively thin cell walls, displaying weak autofluorescence and pale coloration upon lignin staining, are visible at 9 and 14 DAP. They undergo cell wall thickening along with lignin deposition particularly from 14 DAP during the period when C lignin accumulates (Figure 6A) and finally merge with the outer sublayer at 20 DAP. Thus, the inner sublayer may be mainly composed of C lignin.

For selective localization of C lignin, we performed histochemical staining using a nitroso reagent (Figure 6C, the three pictures in the bottom row). Acidic nitrite reacts rapidly with *o*-diphenols to give, when subjected to high pH conditions, reddish chromophores, so the reagent was previously used to visualize catechol metabolites in plant tissues (Reeve, 1959a, 1959b; Kao et al., 2002). As C lignin possesses free catechol moieties as polymer end units, whereas normal G/S lignins do not, the reagent should permit a selective visualization of C lignin produced in *C. hassleriana* seed coats; a preliminary test with DHPs and isolated *C. hassleriana* lignins confirmed that the reaction with C lignins results in diagnostic reddish-brown colorations (see

Supplemental Figure 7 online). In accordance with the lignin compositional analysis by thioacidolysis (Figure 6A), positive reddish-brown coloration for C-lignin had not appeared in the seed coats at 9 and 14 DAP but was clearly evident at 20 DAP (Figure 6C). Importantly, the coloration was observed across the two lignified sublayers, indicating that C lignin deposits not only in the inner sublayer but also in the outer sublayer presumably where G lignin is preformed. To further evaluate this, we carefully isolated the outer main sublayer for lignin compositional analysis by thioacidolysis, by removing the inner sublayer and exotestal layers under a microscope. As expected, the isolated outer sublayer still contained a high level of C lignin along with G lignin (see Supplemental Table 2 online). Overall, our data suggest that both G and C lignin deposition successively occurs in the same testa layers during seed coat development in *C. hassleriana*.

## DISCUSSION

The identification of C lignin in seeds of the Euphorbiaceae and Cleomaceae families affirms our earlier contention that C lignins are distributed quite widely in nature (Chen et al., 2012, 2013). Within angiosperms, C lignin has been found, not ubiquitously,

in both monocots (Cactaceae) and dicots (Orchidaceae, Euphorbiaceae, and Cleomaceae). As we previously observed within the Cactaceae (Chen et al., 2013), the lignin composition in seed coats of the Euphorbiaceae and Cleomaceae is likewise quite variable even within members of the same genus (Figure 1). Thus, unlike ubiquitous G lignin deposition in xylem tissues of tracheophytes (Weng and Chapple, 2010), it is most plausible that C lignin deposition in seed coats is a recently acquired trait. Many of the Euphorbiaceae plants characterized in this study, for example, *J. curcas*, *V. fordii* (also known as the tung oil tree), *A. moluccana* (candlenut), and *R. communis* (castor oil plant), have attracted considerable research attention for their potential applications as feedstocks for biodiesel production (Sujatha et al., 2008; Vega-Sánchez and Ronald, 2010; Abdulla et al., 2011). Studies describing chemical and/or even NMR analysis of seed coats in these plants have consequently been reported recently by other groups (Klein et al., 2010; Martin et al., 2010; Watanabe et al., 2012; Wever et al., 2012; Yamamura et al., 2012). However, the presence of C lignin in the seed coats has remained unclear, possibly because the notion that polymers could result from caffeoyl alcohol polymerization has only been recently recognized (Chen et al., 2012).

The plants identified in our previous studies possess C lignin or G/S lignins in their seed coats, but never both (Chen et al., 2012, 2013). By contrast, lignins in the seed coats of the currently studied members of the Euphorbiaceae and Cleomaceae are composed of C, G, and S units, or C and G units, as clearly evident from thioacidolysis and two-dimensional NMR analysis (Figures 1 and 2). This discovery raised the question as to whether these seeds contain heterogeneous mixtures of C lignin and classical G/S lignins that are biosynthesized independently of each other or homogeneous copolymers that are produced via concurrent copolymerization of the lignin precursors. Our NMR data here clearly show that the former is a general case. HMBC experiments provided no evidence of putative linkages derived via cross-coupling between caffeoyl alcohol and the conventional monolignols in plant seed lignins nor any evidence that the conventional monolignols cross-couple with catechyl units (Figures 4B and 4C). By contrast, such cross-unit linkages were readily produced in vitro via peroxidase-catalyzed copolymerization from the precursor mixtures (Figures 4B and 4C). Thus, in vivo synthesis and polymerization of the caffeoyl alcohol precursor must be spatially and/or temporally separated from that of the conventional monolignols. In accordance with this, the deposition of G and C lignins and the syntheses of their precursors in *C. hassleriana* seed coats are temporally separated during seed maturation; C lignin appears after G lignin deposition (Figure 6A).

Seed coat development is generally a complex process involving differentiation of the ovule integuments into several tissue layers composed of different specialized cells (Haughn and Chaudhury, 2005; Debeaujon et al., 2007). Our microscopy investigations suggest that the *C. hassleriana* seed coat ultimately develops a single continuous layer of cells producing thick lignified cell walls (Figure 6C). It is apparently composed of two sublayers of different cell types that undergo cell wall thickening and lignification at different times during maturation. Taken together with the lignin compositional analysis (Figure 6A), the inner sublayer may accumulate C lignin predominantly after G lignin

appears in the outer sublayer. However, our histochemical analysis using a nitroso reagent to selectively localize C lignin strongly suggests that a certain level of C lignin is also present together with G lignin in the outer sublayers in the mature seed (Figure 6C). Thus, the biosynthesis of G and C lignins, at least the final assembly of the polymers, is likely to occur within the outer sublayers, although there still remains a possibility that C lignin (or the caffeoyl alcohol precursor, further discussed below) biosynthesized in the inner sublayer may later diffuse to the outer sublayer where G lignin has been preformed.

Previous studies on seed development, mainly in *Arabidopsis*, have described biogenesis of phenolic metabolites, such as flavonoids, suberin, and cutin in seeds (Haughn and Chaudhury, 2005; Lepiniec et al., 2006; Debeaujon et al., 2007; Arsovski et al., 2010; North et al., 2010). However, little attention has been paid to seed-specific regulation of lignin biosynthesis. Based on the currently accepted biochemical pathway to monolignols (Umezawa, 2010), caffeoyl alcohol would be formed if the first OMT in the monolignol pathway, CCoAOMT (see Supplemental Figure 1 online), became depleted or lost its function. In fact, downregulation of a gene encoding CCoAOMT in a gymnosperm, *Pinus radiata*, introduced caffeoyl alcohol into lignification, generating low levels of C units in dominant G lignins in the tracheary elements (Wagner et al., 2011). Similarly, downregulation of the second OMT, COMT (see Supplemental Figure 1 online), generates cell wall lignins with unusual 5H units derived from 5-hydroxyconiferyl alcohol (Ralph et al., 2001b; Lu et al., 2010; Vanholme et al., 2010b; Weng et al., 2010). In accordance with the theory and previous studies on OMT-deficient transgenic plants, the abrupt transition of lignins (i.e., from G to C lignins) in developing *C. hassleriana* seed coats is well synchronized with the apparent loss of OMT activities (Figures 6A and 6B). Thus, if the syntheses of caffeoyl alcohol and coniferyl alcohol could be regulated within the same cells, a currently unknown mechanism may allow for a silencing of OMT expression within the seed coat, consequently directing the metabolic flow toward the caffeoyl alcohol precursor and producing C lignin in specific cells at specific developmental stages. It remains intriguing to contemplate how the plant cells accomplish this apparently abrupt transition to no methylation activity with no detectable products of a transition between the two states. If the deposition order had been reversed (i.e., if C lignin deposited before G/S lignin), a simple introduction of new enzymatic activity would suffice, but the reverse order implies that somehow plant cells abruptly cease exhibiting OMT activity or activity of some other enzymes necessary for formation of C1 methyl precursors; the former case is strengthened because we observed the depletion of apparent OMT activities in in vitro assays using added S-adenosyl-L-Met cofactor (see Methods).

Although the above scenario seems to be supported by the OMT activity data over the period of seed development in *C. hassleriana*, other explanations still cannot be excluded without further rigorous genetic investigations. For instance, caffeoyl alcohol and conventional monolignol precursors may simply be synthesized in different cells and transported to the same polymerization sites at different times during seed maturation. As our data suggest that C lignin deposits predominantly in the inner sublayers adjacent to the outer sublayers that accumulate both G and C lignins in *C. hassleriana* seeds, caffeoyl alcohol may be

synthesized specifically in the inner sublayer and diffuse and be polymerized into C lignin in the outer sublayers after coniferyl alcohol has been polymerized into G lignin. It has been shown that the parenchymatic xylem cells that surround tracheary elements have the capacity to synthesize and transport lignin monomers and reactive oxygen species to the cell walls of dead tracheary elements in *Zinnia* (Pesquet et al., 2013). Therefore, it is also possible that caffeyl alcohol and conventional monolignol precursors could be synthesized in different parenchyma cells adjacent to the lignifying cell layers and supplied separately to the lignifying cell layers. Alternatively, regardless of whether caffeyl alcohol and conventional monolignol precursors are synthesized at the same or different locations, it is possible that their syntheses are controlled by different regulatory networks that involve the same enzymes (except OMTs) but not necessarily the same genes; this possibility cannot be easily addressed until genomic data become available for species that synthesize C lignin. Finally, it is still plausible that the G/S and C lignins could be in totally separated cells or cell layers, although we could not unambiguously distinguish such locations at least in *C. hassleriana* seed coats.

The high levels of lignin polymers in the seed coats (total 50 to 70% by Klason analysis; Table 1) support the earlier contention that their primary function is structural, providing mechanical strength and impermeability to the seed coats (Chen et al., 2012). Similarly as proposed for flavonoids (Dixon et al., 2005; Lepiniec et al., 2006), those lignins may additionally provide protection for seeds against microbial pathogens and other biotic and abiotic stresses. Currently, however, it is unknown why these plants biosynthesize the two distinctively different types of lignin polymers (i.e., G/S lignin and C lignins) together within the same testa layers; this seems to imply that C lignin is not simply a replacement for traditional G/S lignins and may potentially have a distinct physiological function. The physicochemical properties and potential effects of lignins on embryogenesis, seed fitness, dormancy, and germination remain elusive.

In summary, the coexistence of independently biosynthesized C lignin and classical G/S lignins in plant seeds exemplifies the flexible but substantially organized manner in which monomers are generated for lignin polymer assembly in nature. A major challenge in current lignin bioengineering is achieving tight regulation of precursor synthesis to enable the flexible design of cell wall lignins with controlled structures (Weng et al., 2008; Vanholme et al., 2012; Bonawitz and Chapple, 2013). In this direction, future studies may focus on understanding the molecular genetic mechanisms that regulate the spatio-temporally specific production of C lignin and the apparently abrupt cessation of O-methylation activity.

## METHODS

### Plant Materials

*Jatropha curcas*, *Aleurites moluccana*, *Vernicia fordii*, *Ricinus communis* and *Cleome hassleriana* seeds were obtained from commercial vendors. The other seeds (listed in Figure 1) were obtained from the National Center for Genetic Resources Preservation. *R. communis* stem, leaf, and root materials were obtained from a 4-month-old plant growing in the greenhouse at the Noble Foundation, Ardmore, OK. *C. hassleriana* plants were

grown in the same greenhouse in MetroMix 350 soil mix at 30°C during the day and 70 to 80% relative humidity. The flowers were hand-pollinated in June of 2011, and the developing seeds were harvested periodically after pollination. Seed coats were preground, and extractives and any remaining seed embryo were removed. The cell wall fraction was then prepared by extraction with chloroform/methanol (2:1, v/v), 100% methanol, and water (three times each), then freeze-dried. For isolation of the main sublayer of *C. hassleriana* seed coats (see the text above), the inner sublayer of the mature seed coats was carefully removed using a surgical knife under a microscope.

### Chemical Analyses

Analytical thioacidolysis was according to the method described previously (Lapierre et al., 1985, 1986). Briefly, ~10 mg of freeze-dried samples were reacted with 3 mL of 0.2 M BF<sub>3</sub>-etherate in an 8.75:1 dioxane/ethanethiol mixture at 100°C for 4 h. Released lignin monomers were extracted with dichloromethane, derivatized with *N,O*-bis(trimethylsilyl)trifluoroacetamide + 1% tetramethylchlorosilane (Pierce Biotechnology), and then subjected to gas chromatography–mass spectrometry analysis on a Hewlett-Packard 5890 series II gas chromatograph with a 5971 series mass-selective detector and HP-1 column (60 m × 0.25 mm, 0.25-μm film thickness). Lignin monomers were quantified using docosane as internal standard. Klason lignin analysis and determination of ash contents were according to the literature method (Hatfield et al., 1994). The distribution of amorphous sugars (hemicelluloses and pectins) and crystalline glucan (cellulose) was calculated by treating the plant material with trifluoroacetic acid and analyzing the amorphous sugars, as alditol acetates, by gas chromatography–mass spectrometry with inositol as internal standard (Albersheim et al., 1967). The residue was washed with the Updegraff reagent (Updegraff, 1969), stripped of further hemicelluloses and amorphous glucan, totally hydrolyzed with sulfuric acid, and Glc quantified by the anthrone assay (Selvendran and O'Neill, 1987). All the analyses were repeated at least twice.

### Whole Cell Wall Dissolution and Acetylation

The cell wall preparations from selected seed samples (*J. curcas*, *V. fordii*, *A. moluccana*, and *C. hassleriana*) were completely dissolved and acetylated using the DMSO/*N*-methylimidazole solvent system as described previously (Lu and Ralph, 2003; Mansfield et al., 2012). Briefly, seed coat preparations (~100 mg) were ball-milled (3 × 20 min, 10-min cooling cycle) using a Retsch PM100 ball-mill vibrating at 600 rpm with ZrO<sub>2</sub> vessels containing ZrO<sub>2</sub> ball bearings. The ball-milled seed tissue (~40 mg) was dissolved in DMSO/*N*-methylimidazole (2:1, v/v, 3 mL) at room temperature. Acetylation was via direct addition of acetic anhydride (1 mL). After stirring for 2 h at room temperature, the mixture was poured into distilled water (1 liter). The resultant precipitate was recovered by filtration, washed with ultrapure water (1 liter), and then lyophilized to yield acetylated seed tissues (weight yields typically at 119 to 141%).

### Isolation of Dioxane-Water-Soluble Lignins

Preextracted and ball-milled seed cell wall preparations (950 mg, *J. curcas*; 1350 mg, *V. fordii*; 1550 mg, *A. moluccana*; 665 mg, *C. hassleriana*) were placed in centrifuge tubes and digested at 30°C with crude cellulases (Cellulysin; Calbiochem; 30 mg/g of sample, in pH 5.0 acetate buffer; three times over 2 d; fresh buffer and enzyme added each time), leaving all of the phenolic polymers and small amounts of residual polysaccharides. The cellulase-treated seed coats were then suspended in dioxane-water (96:4, v/v ~50 mL/g) and stirred at 30°C for 6 h. The mixture was centrifuged (10,000g, 15 min) and the supernatant was collected. These operations were repeated three times. The combined supernatant was concentrated to ~5 mL using a rotary evaporator and then precipitated into 200 mL of 0.01

M aqueous HCl. The precipitates were collected by centrifugation, reprecipitated into diethyl ether (100 mL) from methanol-dichloromethane (1:4, v/v, ~5 mL), and recovered by centrifugation to yield purified dioxane-water-soluble lignins (380 mg, 40%, *Jatropha*; 739 mg, 55%, *Vernicia*; 556 mg, 36%, *Aleurites*; 665 mg, 23%, *C. hassleriana*). Acetylation of the isolated lignins was via acetic anhydride and pyridine: ~50 mg of isolated lignins was dissolved in acetic anhydride/pyridine (1:1, v/v, 2 mL). After stirring at room temperature overnight, the mixture was poured into distilled water (200 mL). The resultant precipitate was recovered by filtration, washed with ultrapure water (200 mL), and then lyophilized to yield acetylated lignins (weight yield typically 117 to 122%).

### Synthetic Lignin Polymers

DHPs from coniferyl alcohol (G-DHP), caffeoyl alcohol (C-DHP), and caffeoyl alcohol in combination with coniferyl alcohol (G/C-DHP) and with coniferyl and sinapyl alcohols (G/S/C-DHP) were generated via horseradish peroxidase-catalyzed polymerization (Tobimatsu et al., 2011; Chen et al., 2012; Tobimatsu et al., 2012): 240 mL of acetone/sodium phosphate buffer (0.1 M, pH 6.5) (1:9, v/v) containing the precursors (coniferyl alcohol or caffeoyl alcohol 1.0 mmol for G-DHP or C-DHP; caffeoyl/coniferyl/sinapyl alcohols = 0.4/0.6/0.0 mmol for G/C-DHP; 0.4/0.3/0.3 mmol for G/S/C-DHP), and a separate solution of hydrogen peroxide (1.2 mmol) in 240 mL of water were added by peristaltic pump over a 20-h period at 25°C to 60 mL of buffer containing horseradish peroxidase (Sigma-Aldrich; type VI, 250 to 330 units, 5 mg). The reaction mixture was further stirred for 4 h and then acidified to pH ~3 with 1 N aqueous HCl solution. The precipitate was collected by centrifugation (10,000g, 15 min), washed with ultrapure water (100 mL × 3), and lyophilized (weight yield 83%, G-DHP; 59%, C-DHP; 64%, G/C-DHP; 36%, G/S/C-DHP). Acetylation of DHPs (~40 mg) was via a standard protocol using acetic anhydride and pyridine as described for acetylation of isolated seed lignins (weight yield 112%, G-DHP; 114%, C-DHP; 116%, G/C-DHP; 109%, G/S/C-DHP).

### NMR Spectroscopy

NMR spectra were acquired on a Bruker Biospin AVANCE 500-MHz spectrometer fitted with a cryogenically cooled 5-mm TCI gradient probe with inverse geometry (proton coils closest to the sample) and spectral processing used Bruker's Topspin 3.1 (Mac) software. Acetylated samples of whole cell walls, isolated lignins, and DHPs were dissolved in chloroform-*d*, and the central chloroform peaks were used as internal reference ( $\delta_C/\delta_H$ : 77.0/7.26 ppm). Adiabatic HSQC experiments (hsqcetgpsisp2.2) were performed using the parameters described previously (Mansfield et al., 2012). Processing used typical matched Gaussian apodization in F2 (LB = -0.5, GB = 0.001) and squared cosine-bell and one level of linear prediction (32 coefficients) in F1. For quantification of aromatic distributions (Figures 2 and 3), linear prediction was turned off, the carbon-2 correlation from G, the carbon-2/6 correlation from S, and the carbon-2 correlation from C units were volume integrated, and the S integrals were logically halved. For an estimation of the various interunit linkage types, the well-resolved side-chain  $C_\alpha$ - $H_\alpha$  contours (**I**<sub>α</sub>, **II**<sub>α</sub>, **III**<sub>α</sub>, and **IV**<sub>α</sub>), or because of spectral overlap of the **IV**<sub>α</sub> contours with carbohydrate signals in whole cell wall NMR (Figure 2), the  $C_\beta$ - $H_\beta$  (**IV**<sub>β</sub>) signals, were integrated; no correction factors were used. The HMBC experiments (hmbcgpplndqf) for isolated lignins and DHP samples had the parameters described previously (Chen et al., 2012). Processing to a final matrix of 2k by 1k data points used typical matched Gaussian apodization in F2 (LB, -30; GB, 0.196), squared sine-bell in F1, and one level of linear prediction in F1 (32 coefficients).

### GPC

Acetylated samples of whole cell walls, isolated lignins, DHPs, caffeoyl alcohol (C-monomer), and a benzodioxane dimer from caffeoyl alcohol

(C-dimer) (Chen et al., 2012) were dissolved in dimethylformamide containing 0.1 M lithium bromide (~0.5 mg mL<sup>-1</sup>) and subjected to GPC analysis on a Shimadzu LC-20A LC system equipped with SPD-M20A photodiode array detector using the following conditions: column, Tosoh TSK gel α-M + α-2500; eluent, dimethylformamide with 0.1 M lithium bromide; flow rate, 0.5 mL min<sup>-1</sup>; column oven temperature, 40°C; sample detection, photodiode array response at 280 nm. The molecular mass calibration was via polystyrene standards. The data acquisition and computation used Shimadzu LCsolution version 1.25 software.

### Assay for OMT Activities

About 0.3 to 0.5 g of ground seed tissue was suspended in 3 mL of extraction buffer (100 mM Tris-Cl, pH 7.5, 10% glycerol, 2 mM DTT, and 0.2 mM MgCl<sub>2</sub>). The suspension was kept on ice for 45 min with occasional vortexing. The supernatant was recovered after centrifugation (12,000g for 5 min) and passed through a 0.45-μm low protein binding acrodisc syringe filter (Pall) and then desalted by passing through a PD-10 column (GE-Healthcare) according to the manufacturer's instructions, with the minor modification of collecting only 1.5 mL of eluent by discarding the first 1.5 mL and the last 0.5 mL. The protein concentrations of plant extracts were determined using the Bio-Rad protein assay. Five to 87 μg of protein extracts was incubated at 30°C for 30 min with 100 mM sodium phosphate buffer, pH 7.5 (for CCoAOMT) or pH 7.2 (for COMT), 0.6 mM MgCl<sub>2</sub>, 2 mM DTT (Roche), 0.2 mM (for CCoAOMT) or 0.8 mM (for COMT) S-(5'-adenosyl)-L-Met dihydrochloride (Sigma-Aldrich), and 0.05 mM caffeoyl-CoA (Stöckigt and Zenk, 1975) as CCoAOMT substrate or 0.5 mM 5-hydroxyconiferaldehyde (Chen et al., 2001) as COMT substrate in a final volume of 50 μL. The reactions were stopped by adding 10 μL of 24% w/v trichloroacetic acid, and products were analyzed by HPLC on a Spherisorb ODS2 column (Waters) in a step gradient using 1% phosphoric acid in water and acetonitrile as eluents. Feruloyl-CoA (Stöckigt and Zenk, 1975) and sinapaldehyde (Sigma-Aldrich) were used to construct the calibration curves for CCoAOMT and COMT assays. The seeds from three plants were combined for enzyme assays, with three repeats.

### Microscopic Lignin Localization

*C. hassleriana* seed samples were fixed with 2.5% (v/v) glutaraldehyde and 4% (v/v) paraformaldehyde in PBS buffer, pH 7.4, postfixed with 1% (v/v) osmium tetroxide for 2 h on ice, dehydrated in a graded ethanol series, and embedded in LR White resin (London Resin). The resin was polymerized at 55°C for 3 d. Serial 1-μm sections were cut with a diamond knife on a Leica EM UC7 ultramicrotome (Leica Mikrosysteme), stained with 1% (w/v) toluidine blue O, phloroglucinol/HCl (2 volumes of 2% [w/v] phloroglucinol in 95% ethanol plus 1 volume of concentrated HCl), or nitroso reagent (1 volume of 10% sodium nitrite, 1 volume of 20% urea, 1 volume of 10% acetic acid, and then 2 volumes of 2 M sodium hydroxide, successively; gas evolution was observed after applications of the first three solutions), and then observed with a Nikon Optophot-2 microscope (Nikon Instruments). For visualization of total lignin autofluorescence, 1-μm sections were immersed in Citifluor (Electron Microscopy Science) and observed under a Leica TCS SP2 AOBS confocal laser scanning microscope (Leica Microsystems) illuminated with a 405-nm blue diode laser and emission detected at 460 nm. Laser intensity, pinhole, and photomultiplier gain settings were kept constant between specimens.

### Supplemental Data

The following materials are available in the online version of this article.

**Supplemental Figure 1.** Pathway Scheme for Lignin Precursors and Polymer Units.

**Supplemental Figure 2.** Lignin Compositions of Different Organs of *Ricinus communis*.

**Supplemental Figure 3.** Aliphatic Subregions of HSQC NMR Spectra of Seed Coat Lignins.

**Supplemental Figure 4.** Aliphatic Subregions of HSQC NMR Spectra of DHPs.

**Supplemental Figure 5.** Pictures of Cleome Seeds during Maturation.

**Supplemental Figure 6.** Extractable OMT Activities in *Cleome* Seeds Based on Protein Content.

**Supplemental Figure 7.** Pictures of Plant Seed Lignins, and DHP and Catechol Standard Solutions Treated with a Nitroso Reagent.

**Supplemental Table 1.** Molecular Weight Distributions of Plant Seed Coat Lignins and DHPs.

**Supplemental Table 2.** Lignin Compositions of Seed Coat Sublayers Isolated from *Cleome* Seeds.

## ACKNOWLEDGMENTS

We thank the National Center for Genetic Resources Preservation, Agricultural Research Service, USDA for providing the Euphorbiaceae and Cleomaceae seeds, Daphna Havkin-Frenkel for introducing us to *C. hassleriana*, Cliff Foster for carbohydrate analysis, and John Grabber for assistance with Klason lignin analysis. This work was supported in part by the Samuel Roberts Noble Foundation and the U.S. Department of Energy's Great Lakes Bioenergy Research Center and Bioenergy Sciences Center, supported by the Office of Biological and Environmental Research in the Department of Energy Office of Science (DE-FC02-07ER64494 and BER DE-AC05-00OR22725).

## AUTHOR CONTRIBUTIONS

Y.T., F.C., J.N., L.L.E.-T., and L.J. performed experiments. Y.T., F.C., R.A.D., and J.R. designed research, analyzed data, and wrote the article.

Received April 25, 2013; revised June 22, 2013; accepted July 6, 2013; published July 31, 2013.

## REFERENCES

- Abdulla, R., Chan, E.S., and Ravindra, P.** (2011). Biodiesel production from *Jatropha curcas*: A critical review. *Crit. Rev. Biotechnol.* **31**: 53–64.
- Albersheim, P., Nevins, D.J., English, P.D., and Karr, A.** (1967). A method for the analysis of sugars in plant cell-wall polysaccharides by gas-liquid chromatography. *Carbohydr. Res.* **5**: 340–345.
- Arsovski, A.A., Haughn, G.W., and Western, T.L.** (2010). Seed coat mucilage cells of *Arabidopsis thaliana* as a model for plant cell wall research. *Plant Signal. Behav.* **5**: 796–801.
- Bewley, J.D., Bradford, K., Hilhorst, H.M., and Nonogaki, H.** (2013). Structure and Composition. In *Seeds*, J.D. Bewley, K. Bradford, H.M. Hilhorst, and H. Nonogaki, eds (New York: Springer), pp. 1–25.
- Björkman, A.** (1954). Isolation of lignin from finely divided wood with neutral solvents. *Nature* **174**: 1057–1058.
- Boerjan, W., Ralph, J., and Baucher, M.** (2003). Lignin biosynthesis. *Annu. Rev. Plant Biol.* **54**: 519–546.
- Bonawitz, N.D., and Chapple, C.** (2010). The genetics of lignin biosynthesis: Connecting genotype to phenotype. *Annu. Rev. Genet.* **44**: 337–363.
- Bonawitz, N.D., and Chapple, C.** (2013). Can genetic engineering of lignin deposition be accomplished without an unacceptable yield penalty? *Curr. Opin. Biotechnol.* **24**: 336–343.
- Carpita, N.C.** (2012). Progress in the biological synthesis of the plant cell wall: New ideas for improving biomass for bioenergy. *Curr. Opin. Biotechnol.* **23**: 330–337.
- Cathala, B., Saake, B., Faix, O., and Monties, B.** (2003). Association behaviour of lignins and lignin model compounds studied by multidetector size-exclusion chromatography. *J. Chromatogr. A* **1020**: 229–239.
- Chen, F., and Dixon, R.A.** (2007). Lignin modification improves fermentable sugar yields for biofuel production. *Nat. Biotechnol.* **25**: 759–761.
- Chen, F., Kota, P., Blount, J.W., and Dixon, R.A.** (2001). Chemical syntheses of caffeoyl and 5-OH coniferyl aldehydes and alcohols and determination of lignin O-methyltransferase activities in dicot and monocot species. *Phytochemistry* **58**: 1035–1042.
- Chen, F., Tobimatsu, Y., Havkin-Frenkel, D., Dixon, R.A., and Ralph, J.** (2012). A polymer of caffeoyl alcohol in plant seeds. *Proc. Natl. Acad. Sci. USA* **109**: 1772–1777.
- Chen, F., Tobimatsu, Y., Jackson, L., Nakashima, J., Ralph, J., and Dixon, R.A.** (2013). Novel seed coat lignins in the Cactaceae: Structure, distribution and implications for the evolution of lignin diversity. *Plant J.* **73**: 201–211.
- Debeajon, I., Lepiniec, L., Pourcel, L., and Routaboul, J.M.** (2007). Seed coat development and dormancy. In *Annual Plant Reviews: Seed Development, Dormancy and Germination*, Vol. 27, K.J. Bradford and H. Nonogaki, eds (Oxford, U.K.: Blackwell Publishing, Inc.) pp. 25–49.
- Dixon, R.A., Xie, D.Y., and Sharma, S.B.** (2005). Proanthocyanidins—A final frontier in flavonoid research? *New Phytol.* **165**: 9–28.
- Egley, G.H., Paul, R.N., Vaughn, K.C., and Duke, S.O.** (1983). Role of peroxidase in the development of water-impermeable seed coats in *Sida spinosa* L. *Planta* **157**: 224–232.
- Elumalai, S., Tobimatsu, Y., Grabber, J.H., Pan, X., and Ralph, J.** (2012). Epigallocatechin gallate incorporation into lignin enhances the alkaline delignification and enzymatic saccharification of cell walls. *Biotechnol. Biofuels* **5**: 59.
- Faix, O., Lange, W., and Besold, G.** (1981). Molecular-weight determinations of DHPs from mixtures of precursors by steric exclusion chromatography (HPLC). *Holzforschung* **35**: 137–140.
- Hatfield, R.D., Jung, H.G., Ralph, J., Buxton, D.R., and Weimer, P.J.** (1994). A comparison of the insoluble residues produced by the Klason lignin and acid detergent lignin procedures. *J. Sci. Food Agric.* **65**: 51–58.
- Haughn, G., and Chaudhury, A.** (2005). Genetic analysis of seed coat development in *Arabidopsis*. *Trends Plant Sci.* **10**: 472–477.
- Holtman, K.M., Chang, H.M., and Kadla, J.F.** (2007). An NMR comparison of the whole lignin from milled wood, MWL, and REL dissolved by the DMSO/NMI procedure. *J. Wood Chem. Technol.* **27**: 179–200.
- Kao, Y.Y., Harding, S.A., and Tsai, C.J.** (2002). Differential expression of two distinct phenylalanine ammonia-lyase genes in condensed tannin-accumulating and lignifying cells of quaking aspen. *Plant Physiol.* **130**: 796–807.
- Kelly, K.M., Vanstaden, J., and Bell, W.E.** (1992). Seed coat structure and dormancy. *Plant Growth Regul.* **11**: 201–209.
- Klein, A.P., Beach, E.S., Emerson, J.W., and Zimmerman, J.B.** (2010). Accelerated solvent extraction of lignin from *Aleurites moluccana* (Candlenut) nutshells. *J. Agric. Food Chem.* **58**: 10045–10048.
- Lapierre, C., Monties, B., and Rolando, C.** (1985). Thioacidolysis of lignin: Comparison with acidolysis. *J. Wood Chem. Technol.* **5**: 277–292.
- Lapierre, C., Monties, B., and Rolando, C.** (1986). Thioacidolysis of poplar lignins: Identification of monomeric syringyl products and characterization of guaiacyl-syringyl lignin fractions. *Holzforschung* **40**: 113–118.

- Lepiniec, L., Debeaujon, I., Routaboul, J.M., Baudry, A., Pourcel, L., Nesi, N., and Caboche, M.** (2006). Genetics and biochemistry of seed flavonoids. *Annu. Rev. Plant Biol.* **57**: 405–430.
- Liang, M.X., Davis, E., Gardner, D., Cai, X.N., and Wu, Y.J.** (2006). Involvement of *AtLAC15* in lignin synthesis in seeds and in root elongation of *Arabidopsis*. *Planta* **224**: 1185–1196.
- Lu, F., Marita, J.M., Lapierre, C., Jouanin, L., Morreel, K., Boerjan, W., and Ralph, J.** (2010). Sequencing around 5-hydroxyconiferyl alcohol-derived units in caffeic acid O-methyltransferase-deficient poplar lignins. *Plant Physiol.* **153**: 569–579.
- Lu, F., and Ralph, J.** (2003). Non-degradative dissolution and acetylation of ball-milled plant cell walls: High-resolution solution-state NMR. *Plant J.* **35**: 535–544.
- Mansfield, S.D.** (2009). Solutions for dissolution—Engineering cell walls for deconstruction. *Curr. Opin. Biotechnol.* **20**: 286–294.
- Mansfield, S.D., Kim, H., Lu, F., and Ralph, J.** (2012). Whole plant cell wall characterization using solution-state 2D NMR. *Nat. Protoc.* **7**: 1579–1589.
- Marita, J.M., Ralph, J., Hatfield, R.D., Guo, D., Chen, F., and Dixon, R.A.** (2003). Structural and compositional modifications in lignin of transgenic alfalfa down-regulated in caffeic acid 3-O-methyltransferase and caffeoyl coenzyme A 3-O-methyltransferase. *Phytochemistry* **62**: 53–65.
- Marita, J.M., Ralph, J., Lapierre, C., Jouanin, L., and Boerjan, W.** (2001). NMR characterization of lignins from transgenic poplars with suppressed caffeic acid O-methyltransferase activity. *J. Chem. Soc., Perkin Trans.* **2**: 2939–2945.
- Martin, C., Moure, A., Martin, G., Carrillo, E., Dominguez, H., and Parajo, J.C.** (2010). Fractional characterisation of jatropha, neem, moringa, trisperma, castor and candlenut seeds as potential feedstocks for biodiesel production in Cuba. *Biomass Bioenergy* **34**: 533–538.
- Moinuddin, S.G.A., Jourdes, M., Laskar, D.D., Ki, C., Cardenas, C.L., Kim, K.-W., Zhang, D., Davin, L.B., and Lewis, N.G.** (2010). Insights into lignin primary structure and deconstruction from *Arabidopsis thaliana* COMT (caffeic acid O-methyl transferase) mutant *Atomt1*. *Org. Biomol. Chem.* **8**: 3928–3946.
- Morreel, K., Ralph, J., Lu, F., Goeminne, G., Busson, R., Herdewijn, P., Goeman, J.L., Van der Eycken, J., Boerjan, W., and Messens, E.** (2004). Phenolic profiling of caffeic acid O-methyltransferase-deficient poplar reveals novel benzodioxane oligolignols. *Plant Physiol.* **136**: 4023–4036.
- North, H., et al.** (2010). *Arabidopsis* seed secrets unravelled after a decade of genetic and omics-driven research. *Plant J.* **61**: 971–981.
- Pesquet, E., et al.** (2013). Non-cell-autonomous postmortem lignification of tracheary elements in *Zinnia elegans*. *Plant Cell* **25**: 1314–1328.
- Ralph, J., Akiyama, T., Kim, H., Lu, F., Schatz, P.F., Marita, J.M., Ralph, S.A., Reddy, M.S.S., Chen, F., and Dixon, R.A.** (2006). Effects of coumarate 3-hydroxylase down-regulation on lignin structure. *J. Biol. Chem.* **281**: 8843–8853.
- Ralph, J., Lapierre, C., Lu, F., Marita, J.M., Pilate, G., Van Doorselaere, J., Boerjan, W., and Jouanin, L.** (2001a). NMR evidence for benzodioxane structures resulting from incorporation of 5-hydroxyconiferyl alcohol into lignins of O-methyltransferase-deficient poplars. *J. Agric. Food Chem.* **49**: 86–91.
- Ralph, J., et al.** (2001b). Elucidation of new structures in lignins of CAD- and COMT-deficient plants by NMR. *Phytochemistry* **57**: 993–1003.
- Reeve, R.M.** (1959a). Histological and histochemical changes in developing and ripening peaches. III. Catechol tannin content per cell. *Am. J. Bot.* **46**: 645–650.
- Reeve, R.M.** (1959b). Histological and histochemical changes in developing and ripening peaches. I. The catechol tannins. *Am. J. Bot.* **46**: 210–217.
- Rencoret, J., Ralph, J., Marques, G., Gutiérrez, A., Martínez, Á.T., and Del Río, J.C.** (2013). Structural characterization of the lignin from coconut (*Cocos nucifera*) coir fibers. *J. Agric. Food Chem.* **61**: 2434–2445.
- Rolston, M.P.** (1978). Water impermeable seed dormancy. *Bot. Rev.* **44**: 365–396.
- Selvendran, R.R., and O'Neill, M.A.** (1987). Isolation and analysis of cell walls from plant material. *Methods Biochem. Anal.* **32**: 25–153.
- Simmons, B.A., Loqué, D., and Ralph, J.** (2010). Advances in modifying lignin for enhanced biofuel production. *Curr. Opin. Plant Biol.* **13**: 313–320.
- Stewart, J.J., Akiyama, T., Chapple, C.C.S., Ralph, J., and Mansfield, S.D.** (2009). The effects on lignin structure of overexpression of ferulate 5-hydroxylase in hybrid poplar. *Plant Physiol.* **150**: 621–635.
- Stöckigt, J., and Zenk, M.H.** (1975). Chemical syntheses and properties of hydroxycinnamoyl-coenzyme A derivatives. *Z. Naturforsch., C, Biosci.* **30**: 352–358.
- Sujatha, M., Reddy, T.P., and Mahasi, M.J.** (2008). Role of biotechnological interventions in the improvement of castor (*Ricinus communis* L.) and *Jatropha curcas* L. *Biotechnol. Adv.* **26**: 424–435.
- Tobimatsu, Y., Davidson, C.L., Grabber, J.H., and Ralph, J.** (2011). Fluorescence-tagged monolignols: Synthesis, and application to studying *in vitro* lignification. *Biomacromolecules* **12**: 1752–1761.
- Tobimatsu, Y., Elumalai, S., Grabber, J.H., Davidson, C.L., Pan, X., and Ralph, J.** (2012). Hydroxycinnamate conjugates as potential monolignol replacements: *In vitro* lignification and cell wall studies with rosmarinic acid. *ChemSusChem* **5**: 676–686.
- Tobimatsu, Y., Takano, T., Kamitakahara, H., and Nakatsubo, F.** (2006). Studies on the dehydrogenative polymerizations of monolignol  $\beta$ -glycosides. Part 2: Horseradish peroxidase catalyzed dehydrogenative polymerization of isoconiferin. *Holzforschung* **60**: 513–518.
- Umezawa, T.** (2010). The cinnamate/monolignol pathway. *Phytochem. Rev.* **9**: 1–17.
- Updegraff, D.M.** (1969). Semi micro determination of cellulose in biological materials. *Anal. Biochem.* **32**: 420–424.
- Vanholme, R., Demedts, B., Morreel, K., Ralph, J., and Boerjan, W.** (2010a). Lignin biosynthesis and structure. *Plant Physiol.* **153**: 895–905.
- Vanholme, R., Morreel, K., Darrach, C., Oyarce, P., Grabber, J.H., Ralph, J., and Boerjan, W.** (2012). Metabolic engineering of novel lignin in biomass crops. *New Phytol.* **196**: 978–1000.
- Vanholme, R., Morreel, K., Ralph, J., and Boerjan, W.** (2008). Lignin engineering. *Curr. Opin. Plant Biol.* **11**: 278–285.
- Vanholme, R., Ralph, J., Akiyama, T., Lu, F., Rencoret Pazo, J., Christensen, J., Rohde, A., Morreel, K., DeRycke, R., Kim, H., Van Reusel, B., and Boerjan, W.** (2010b). Engineering traditional monolignols out of lignins by concomitant up-regulation *F5H1* and down-regulation of *COMT* in *Arabidopsis*. *Plant J.* **64**: 885–897.
- Vega-Sánchez, M.E., and Ronald, P.C.** (2010). Genetic and biotechnological approaches for biofuel crop improvement. *Curr. Opin. Biotechnol.* **21**: 218–224.
- Vogt, T.** (2010). Phenylpropanoid biosynthesis. *Mol. Plant* **3**: 2–20.
- Wagner, A., Tobimatsu, Y., Phillips, L., Flint, H., Torr, K.M., Donaldson, L., Pears, L., and Ralph, J.** (2011). CCoAOMT suppression modifies lignin composition in *Pinus radiata*. *Plant J.* **67**: 119–129.
- Watanabe, T., Shino, A., Akashi, K., and Kikuchi, J.** (2012). Spectroscopic investigation of tissue-specific biomass profiling for *Jatropha curcas* L. *Plant Biotechnol.* **29**: 163–170.

- Weng, J.K., and Chapple, C.** (2010). The origin and evolution of lignin biosynthesis. *New Phytol.* **187**: 273–285.
- Weng, J.K., Li, X., Bonawitz, N.D., and Chapple, C.** (2008). Emerging strategies of lignin engineering and degradation for cellulosic biofuel production. *Curr. Opin. Biotechnol.* **19**: 166–172.
- Weng, J.-K., Mo, H., and Chapple, C.** (2010). Over-expression of F5H in COMT-deficient *Arabidopsis* leads to enrichment of an unusual lignin and disruption of pollen wall formation. *Plant J.* **64**: 898–911.
- Wever, D.A.Z., Heeres, H.J., and Broekhuis, A.A.** (2012). Characterization of Physic nut (*Jatropha curcas* L.) shells. *Biomass Bioenergy* **37**: 177–187.
- Yamamura, M., Akashi, K., Yokota, A., Hattori, T., Suzuki, S., Shibata, D., and Umezawa, T.** (2012). Characterization of *Jatropha curcas* lignins. *Plant Biotechnol.* **29**: 179–183.
- Yue, F., Lu, F., Sun, R., and Ralph, J.** (2012). Synthesis and characterization of new 5-linked pinoresinol lignin models. *Chemistry* **18**: 16402–16410.

